COMPUTER MODELLING OF MONTSERRAT GEOTHERMAL FIELD

Ulysse Lehuger[1], Mike O'Sullivan[1], John O'Sullivan[1], Joris Popineau[1] and Graham A. Ryan[2]

[1]Department of Engineering Science, University of Auckland, Auckland, New Zealand

[2] Seismic Research Centre, The University of the West Indies, St. Augustine, Trinidad and Tobago, W.I.

m.osullivan@auckland.ac.nz

Keywords: *Montserrat, computer modelling.*

ABSTRACT

A geothermal field on the island of Montserrat is being investigated and considered for development. There have been various geoscientific studies and three wells have been drilled. Temperature profiles are available from two of them. From this information a conceptual model was developed and a computer model was set up. A fairly simple geological model was used with only four major formations and five major faults included.

The model covers an area of 7 km x 6 km and extends to a depth of 4000 m below sea level. An air/water equation of state is used so that the unsaturated vadose zone can be included. Part of the model extends under the ocean. The model contains ~16000 blocks (28 x 24 blocks in most layers, but fewer in the shallow layers that follow the topography and bathymetry).

A natural state model was first manually calibrated and then automated calibration with iTOUGH2 was used to further improve calibration. A good fit to the temperature profiles in Mon-1 and Mon-2 was achieved.

1. INTRODUCTION

Montserrat is a small island located in the Caribbean archipelago (Figure 1). It is a volcanic island with one currently active volcano the Soufrière Hills Volcano, which is located in the south of the island and has been erupting since 1995. The Eastern Caribbean is a geothermal area because it is on the boundary between the Caribbean plate and the South American plate.

Figure 1: Montserrat in the Caribbean

Montserrat and neighbouring islands have significant geothermal energy resources and there is geothermal power plant on Guadeloupe, a neighbouring island (Jaude and Lamethe, 1985).

The electrical power demand for Montserrat is about 2 MWe and the island is dependent on fossil fuel for generating electricity, which has a much higher operational cost than geothermal energy (Ryan and Shalev, 2014) and contributes more carbon dioxide emissions as well as other pollutants.

The government of Montserrat is investigating the possibility of using geothermal energy to replace fossil fuel for electricity generation. In 2009, EGS Inc., a USA geothermal exploration company, was asked by the government to conduct preliminary surveys of geology, geophysics and geochemistry to study the feasibility of developing geothermal electricity in the island.

In a previous study (Sumantoro, 2014) a simple natural state model of Montserrat was set up. In the current study a more detailed model with a finer grid is developed, based on an updated conceptual model. Both manual calibration and automatic calibration with iTOUGH2 (Finsterle, 2007) are used to obtain a model that matches well the measured temperature profiles in wells Mon-1 and Mon-2.

2. CONCEPTUAL MODEL

2.1 Surface features

The island of Montserrat was formed by predominantly andesitic, eruptive activity, starting in the older Silver Hills at the north, shifting to the Centre Hills in the middle of the island and then to the currently active Soufrière and South Soufrière Hills Volcano in the south (EGS, 2010). Located to the west of the Soufrière Hills Volcano are three smaller morphological features, Garibaldi Hill, Richmond Hill and St George's Hill. These features are thought to be related to tectonic uplift and tilting (Harford et al., 2002; Rowland and Ryan, 2014). This area is around the area of interest for the geothermal exploration discussed here.

From the initial surveys (EGS, 2009; Ryan et al., 2013) the area between Garibaldi Hill and St George's Hill was identified as having potential for the development of geothermal energy in Montserrat. There are two different theories about the geological basis for these hills. Rea (1974) concluded Garibaldi Hill is an eruptive centre while Harford et al. (2002) said that the hills were a result of tectonic uplift and tilting. According to EGS (2010), St George's Hill consists of andesitic block and ash-flow deposits, pumice and ash-flow deposits and epiclastic deposits while Garibaldi Hill consists of similar pyroclastic and epiclastic sequences.

2.2 Geology and structural models

Montserrat was formed by predominantly andesitic eruptions, starting in the older Silver Hills at the north. Activity then shifted to the centrally located Centre Hills volcanic complex before moving to the Soufrière Hills and South Soufrière Hills to the south, with the Soufrière Hills Volcano being currently active (Wadge et al., 2014). Garibaldi Hill, Richmond Hill and St George's Hill are three

smaller morphological features on the western side of Soufriere Hills Volcano, which are the area of interest for the geothermal exploration discussed here.

An older study (EGS, 2010) suggested that there are two major faults in Montserrat:

(i) The NNW-SSE trend or Basse Terre – Montserrat Fault, which extends from the south of Montserrat to the west of Guadeloupe.
(ii) The WNW trend or Redonda Fault, which is shown by cliff exposures on both the east and west coast of Montserrat.

In the target area a N-S fault separates Garibaldi Hill and St George's Hill and WNW striking fault at Garibaldi Hill and St George's hill has the same direction as the Redonda fault.

Those faults are represented in Figure 2.

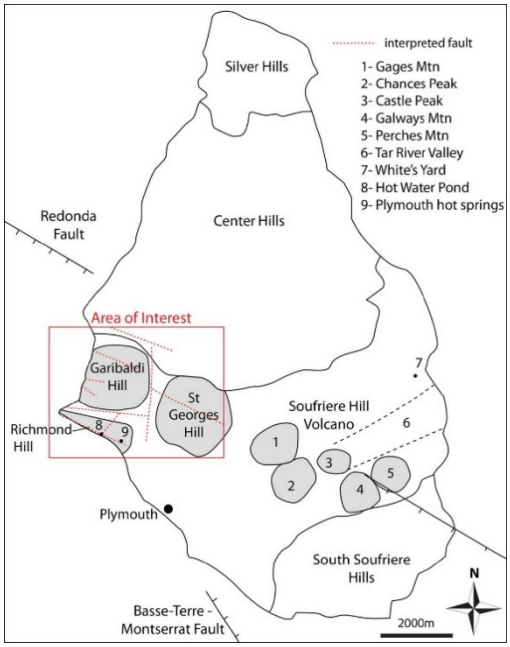

Figure 2: Structural map of Montserrat (modified after EGS, 2010)

A recent study by Rowland and Ryan (2014) carried out reconnaissance structural mapping and identified the structures in the study area shown in Figure 3. They identified the NW striking St. Georges Hill Fault Zone (SGHFZ) as the most impressive structural fabric observed. They also identified a major NE to ENE striking fault, with a dominant down-throw to the SE, strikes along the SE flank of St George's Hill and called it the Fort Ghaut Fault Zone (FGFZ).

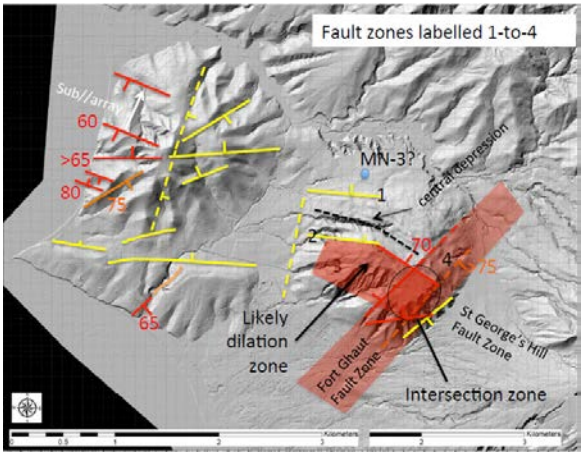

Figure 3: Lineaments in the St George's Hill/Garibaldi Hill Area (from Rowland and Ryan, 2014)
Red- confident. Orange- Some uncertainty with respect to strike, dip or dip direction of controlling structure, dashed if inferred based on nearby field observations. Yellow-unsupported by field data, but likely based on geomorphic expression, dashed if more speculative

2.3 Geophysics

There are several methods that have been utilized for geophysical surveys on Montserrat, such as magneto-telluric (MT), coupled with time domain electromagnetics (TDEM) for resistivity modelling and some analysis of natural seismicity All geophysical surveys were completed by the Institute of Earth Science and Engineering at the University of Auckland, New Zealand (IESE).

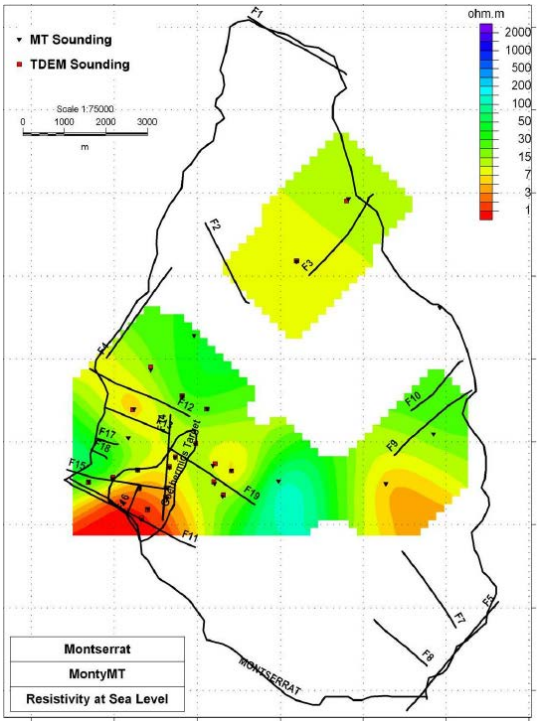

Figure 4: Resistivity map at sea level.

The resistivity map above in Figure 4 shows the low resistivity clay cap, at depths of around 500-1000 meters, alongside Garibaldi Hill to the west of Gage's Mountain at the centre of the island. The dome in the cap beneath St George's Hill may indicate an alteration area due to steam

condensate from a hot upflow along the NW and NE trending fault zones. This is an important feature because this upflow below the clay cap is likely to be the target area for geothermal electricity production.

From the map, a deeper high resistivity area can be found below St George's Hill and Gage's Mountain, which may be interpreted as a solidified pluton/old magma chamber (EGS, 2010) but is more likely an interpretation artefact.

Resistivity maps were also built to assess the spatial distribution of resistivity at different depths. The map at 1000 mbsl shows a low resistivity area that may indicate hydrothermal alteration and fault zones, while the map at 4000 mbsl shows a deep low resistivity area that may be related to a magma chamber beneath the volcano (EGS, 2010) or may be another interpretation artefact.

From the SEA-CALIPSO experiment (an active seismic tomography experiment) it was found that the area around Garibaldi Hill and St George's Hill has a low seismic velocity, and so this area is likely to be a high permeability, fractured zone or an area with high degrees of alteration associated with the high-temperature geothermal system (Shalev et al., 2010; Ryan and Shalev, 2014).

2.4 Geochemistry

From past surveys, all surface manifestations indicate that a long-established geothermal system is present in the southern part of the island. EGS (2010) pointed out that the existence of alkali-chloride thermal springs and several fumarole fields support this conclusion. There is a thermal spring feeding Hot Water Pond, located 1 km from Plymouth, which is the most obvious indication of active hydrothermal activity on Montserrat. This hot spring area consists of several seepages and pools, which have a total outflow of 5 kg/s and a temperature of about 90^{0}C.

2.5 Well data

Two exploration wells were drilled during the drilling campaign in 2013. MON-1 was drilled to a total depth of 2298 m while MON-2 reached the total depth of 2870 m. Flow test data from well MON-1 showed that the mass flow rate reached 22 kg/s and the bottom-hole temperature was 230^{0}C. On the other hand, flow test data from well MON-2 showed that the mass flow rate reached 12 kg/s and the bottom temperature was 265^{0}C (EGS, 2014).

Data from cutting logs in MON-1 indicated a smectite clay zone between 600-1200 m in depth, containing sandstones, mudstones and smectite-containing clays. This area is associated with the low resistivity zone and is interpreted as the reservoir clay cap. Furthermore, the area between 1200-2200 m depth is interpreted as the main reservoir zone (EGS, 2014). MON-2 has a similar lithology to well MON-1.

In Figure 5 there are temperature profiles for MON-1 and MON-2. Both temperature profiles are derived from upwards and downwards going runs of the temperature logging tool. To regularize the data average temperatures where calculated for each 5 m interval and upwards and downwards going temperatures where averaged to reduce the effect of the thermal inertia of the logging tool. The temperature data from Mon-2 showed a significant perturbation in well temperatures between 1325 and 2195 m. This reduction in temperature is thought to be due to incomplete warming up of the well after cooling during the circulation of drilling fluids. To compensate for this perturbation, we calculated a linear temperature fit across the perturbed zone which is thought to approximate the unperturbed reservoir temperatures.

Figure 5: Plots of Temperature vs. Depth for MON-1 and MON-2

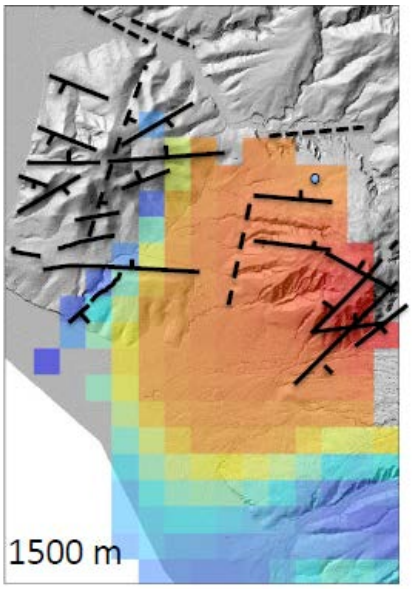

Figure 6: Estimated temperatures at 1500 m depth from a seismic velocity anomaly model (Rowland and Ryan, 2014)

2.6 Integrated model

Based on the seismic tomography work of Ryan and Shalev (2014), Rowland and Ryan (2014) presented the temperature model shown above in Figure 6. They note that the location of the hot spot at 1500 m depth coincides with the intersection of the two major fault zones near St George's Hill, namely the SGHFZ and the FGFZ. However, deeper at 2000 m the hot spot seems to move further NNW closer to the intersection between Fault 2 and SGHFZ

3. COMPUTER MODEL DESIGN

3.1 Model grid

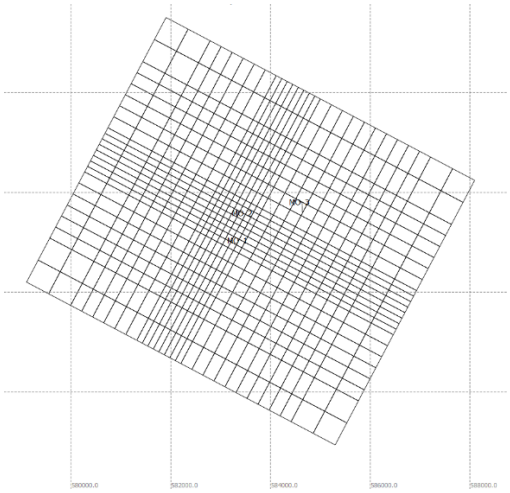

Figure 7: Plan view of the grid for the model of Montserrat (showing locations of wells)

Figure 7 shows the model grid. It is 7 km square, composed of blocks of various sizes: i.e., 500m, 250m or 125m on a side. The grid is finer in the centre where wells Mon-1 and Mon-2 and the geothermal reservoir are located. The coordinates on Figure 7 are from the UTM system. There are 16587 blocks in the model grid, with 30 layers and 672 columns. The base of the model is at -4000m and top is variable, following the topography (see below).

3.2 Topography and bathymetry

Topography of Montserrat was downloaded and pyTOUGH scripts (Croucher 2011, 2015; Wellmann et al. 2012) were used to assign a surface elevation to all columns except those in the ocean whose top was set to match the bathymetry. The bathymetry around Montserrat and the location of the model grid are shown in Figure 8. The red line is the coastline.

An approximate piece-wise constant bathymetry was applied with water depths of 10m, 20m, 50m, 100m or 150m.

Thin layers of 50m or 100m were used in the shallow zone of the model to better represent the topography and bathymetry. A slice through the model is shown in Figure 9.

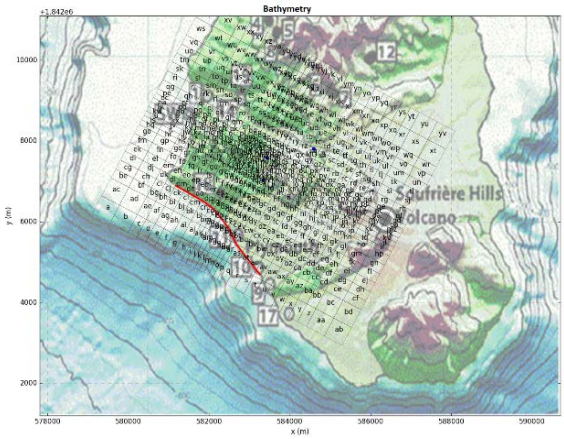

Figure 8: Bathymetry near Montserrat

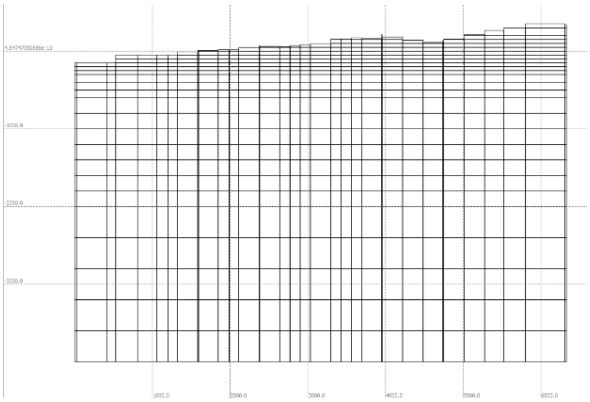

Figure 9: Slice through the model

3.3 Geology and faults

For the model, the geology is approximated as 5 important formations, based on the geophysical surveys and well data. The geophysical surveys show a clay cap between depths, below sea level, of 500m and 1000m, and it is selected as one of the formations. There is another formation corresponding to shallow formations from the surface to the top of the clay cap. Below the clay cap, according to well data and different gradients on the temperature profiles it is possible to identify 3 main formations: one between 1000m and 1600m, another between 1600m and 2000m and the last below 2000m. Each layer have a special name based on its depth.

Table 1: Rock-types in the model

Rock-type name	Layers	Elevations (mrSL
A	1 to 17	700 to -600
B	18-19	-600 to -1000
C	20-22	-1000 to -1600
D	23-24	-1600 to -2000
E	25-29	-2000 to -4000

As shown in Table 1 each formation is assigned a simple identifier.

Figure 10 shows the model grid superimposed on a map of Montserrat.

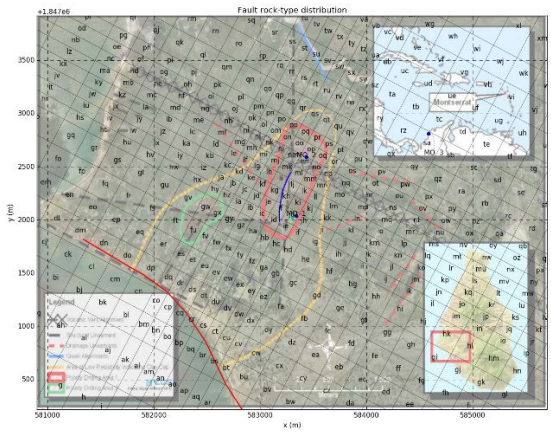

Figure 10: Model grid superimposed on a map of Montserrat

On the basis of this map 5 faults were selected for representation in the model, numbered 1 through 5. Three additional faults (numbered 6-8) were added to correspond to Fault 2, the SGHFZ and the FGFZ (see Fig. 3). The way these faults are represented in the model is shown in Figure 11.

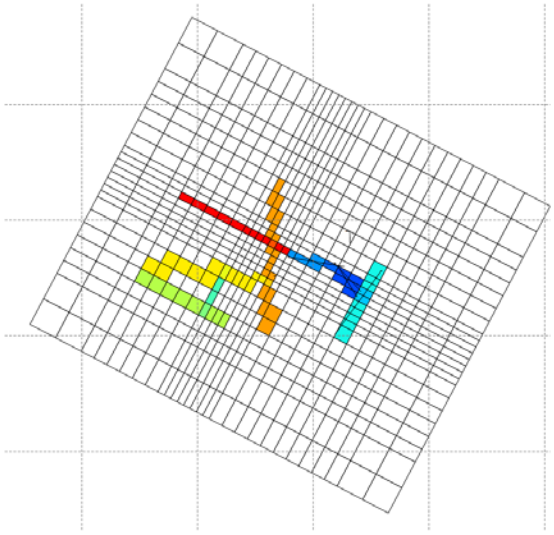

Figure 11: Fault zones in the model of Montserrat

Within each formation 15 rock-types are introduced: 1 for the basic un-faulted formation, 8 for the faults and 6 for the intersection between two faults. Thus in the whole model there are 70 rock-types, and therefore 225 permeabilities (1 in each direction for each rock-type) to be selected by calibration

3.4 Boundary conditions

3.4.1 Base of model

Across the whole of the base of the model a background heat flow of 100 mW/m^2 is set. This is a reasonable value for geothermal area like Montserrat. In addition an upflow of very hot water (1250kJ/kg) was added at some of the fault blocks at the base of the model. The initial locations for the deep hot upflow were determined from the conceptual model, but were adjusted as part of the calibration process.

3.4.2 Sides of model

For the natural state model all sides are treated as closed, i.e., there is no heat or mass transfer across the boundaries. For later production history simulations recharge boundary conditions may be introduced if there are significant pressure changes in the boundary blocks.

3.4.3 Top of model

For the top of the columns located on the island there are two boundary conditions imposed: first, an atmospheric pressure of 1.0135bar, temperature of 28°C and an air mass fraction of 0.999825 (corresponding to almost dry air). Secondly, infiltration of rainfall is represented by injection of water into the top of the model at a rate of 3.171e-5 kg/(m^2.s) at an enthalpy of 117.4kJ/kg (28°C). This infiltration rate corresponds to 10% of the annual rainfall of 1000mm/year.

Under the ocean the pressure at the top of each column is set at the hydrostatic pressure for the depth of the ocean, based on a fresh water density of 996.2 kg/m^3 and the temperature is set at 28°C. Note that an approximation is made and the sea is treated as fresh water. It would be better to use the EWASG equation of state which allows simulations with mixtures of water, NaCl and air, however models with this EOS tend to run more slowly than with the equation of state EOS3 (air/water) used here.

4. NATURAL STATE MODEL

4.1 Manual calibration

In the first version of the model, parameters from the earlier model set up by Sumantoro (2014) were used as a starting point and then they were manually adjusted to improve the fit of the model results to the downhole temperature profiles in Mon-1 and Mon-2.

The general principles followed were:

(i) The permeability in the clay cap is lower than in the other formations.
(ii) The permeability in the faults is larger than in the host rock.

For manual calibration the structure of the deep upflow was kept simple by specifying the same rate in each of the upflow blocks.

Figure 12 presents result of an early stage of manual calibration. The match for Mon-1 is reasonable but the match for Mon-2 is not good enough.

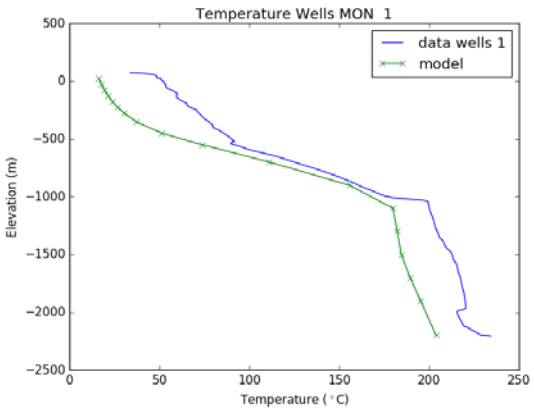

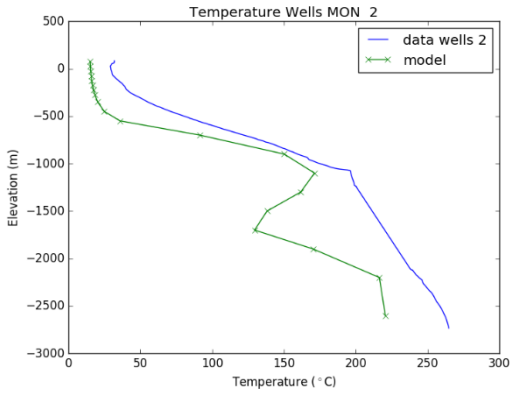

Figure 12: Results at an early stage of manual calibration

4.2 Calibration with iTOUGH2

In parallel with improving manual calibration it was decided to use iTOUGH2 (Finsterle, 2007) to carry out automatic calibration. For the observations to be matched the downhole temperature profiles for Mon-1 and Mon-2 were interpolated on to layer centres, giving a total of 39 data points, then 3 surface temperatures were added for zones of surface activity giving a total of 42 observations. The adjustable parameters used were 225 permeabilities (3 for each rock-type) and flow rates at 31 upflow blocks, giving a total of 256 parameters.

After some experimentation in setting up and lower bounds on the model parameters it was possible to achieve a successful simulation with iTOUGH2. With 4 parameter updates, each taking 257 forward simulations with TOUGH2, a 75% reduction in the objective function was achieved. The objective function is a measure of the calibration of the model, calculated as a sum of squares of the difference be the observations and the model results.

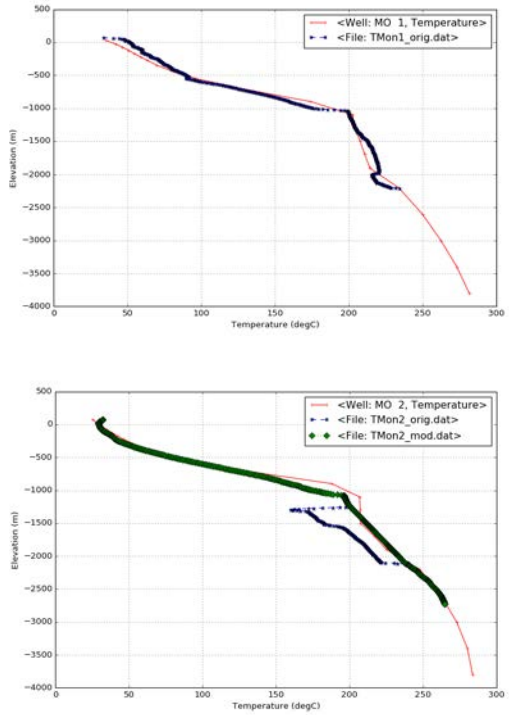

Figure 13: Results after calibration with iTOUGH2

Figure 13 shows the good match achieved to the down-hole temperatures in wells Mon-1 and Mon-2.

The post-calibration permeability (k1, in the SW-NE direction) in the top (A) formation is shown in Figure 14. The same results for formations B-E are shown in Figures 15-18, respectively. Similar plots for K2 and k3 could also be produced.

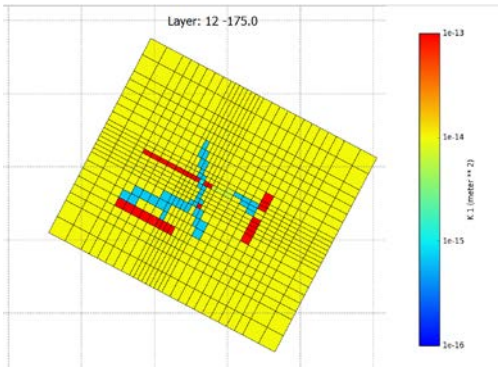

Figure 14: Post-calibration k1 permeability in A formation

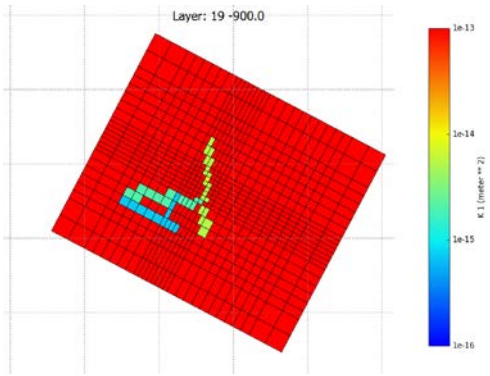

Figure 15: Post-calibration k1 permeability in B formation

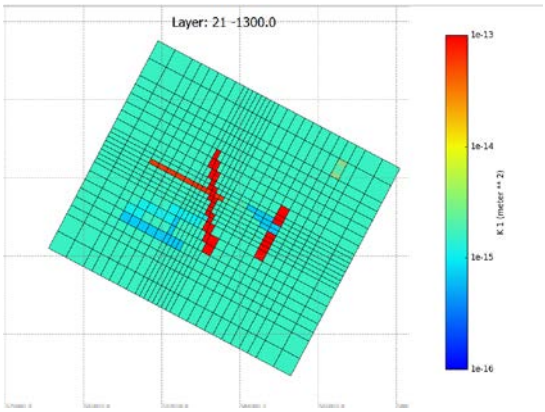

Figure 16: Post-calibration k1 permeability in C formation

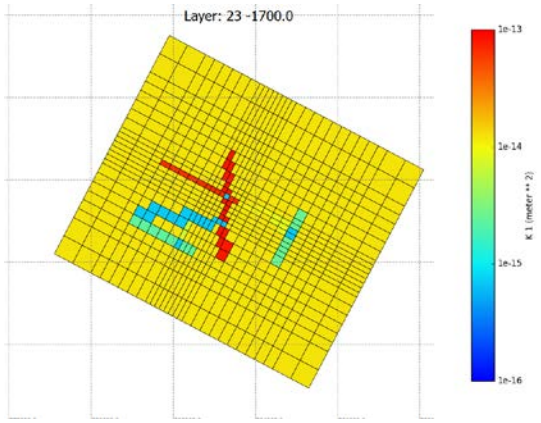

Figure 17: Post-calibration k1 permeability in D formation

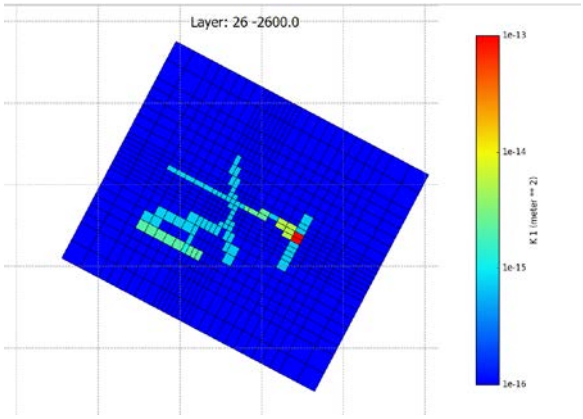

Figure 18: Post-calibration k1 permeability in E formation

Some of the permeabilities shown in Figures 14-18 may be misleading because iTOUGH2 tends to push poorly constrained parameters towards either their upper or lower bounds. Thus in some cases a very low or very high value for k1 for a particular rock-type may not be meaningful – it may merely indicate that the parameter concerned is not well determined by the data and a model with a different value of the particular parameter would fit the observations just as well. Table 2 give information extracted from the "status" file generated by iTOUGH2 for the 23 least constrained parameters, indicated by a sensitivity less than 0.01. It shows that all except one parameter (k1 for FEE78) is at the lower bound (-15.15) or upper bound (-11.50). Note that the permeability parameters are taken as log10 of permeabilities. In the future these parameters should be removed from the suite to be optimised by iTOUGH2 and their values set at some reasonable default.

Table 2: Poorly constrained model parameters

Rock-type	Perm.	Value	Sensitivity
FDD66	k1	-15.15	0.008
FBB68	k2	-15.15	0.006
FEE78	k1	-14.11	0.005
FAA77	k2	-15.15	0.005
FAA12	k3	-11.50	0.003
FDD78	k2	-15.15	0.002
FAA66	k1	-11.50	0.001
FBB23	k1	-11.50	0.001
FDD68	k1	-11.50	0.001
FAA78	k2	-15.15	0.001
FBB66	k2	-15.15	0.001
FAA68	k1	-11.50	0
FAA88	k2	-11.50	0
FCC23	k1	-11.50	0
FCC66	k1	-11.50	0
FCC77	k2	-11.50	0
FCC78	k2	-11.50	0
FCC88	k2	-11.50	0
FDD44	k2	-11.50	0
FDD23	k2	-11.50	0
FDD45	k2	-11.50	0
FDD68	k2	-11.50	0
FDD11	k2	-15.15	0

The values of the deep upflows selected by iTOUGH2 are shown in Figure 19. The upflow under St. George's Hill is low but the sensitivities for the upflows there are one or two orders of magnitude less than the sensitivities for the upflows near Mon-1 and Mon-2 thus indicating that the upflow under St. George's Hill is poorly constrained by the observations available.

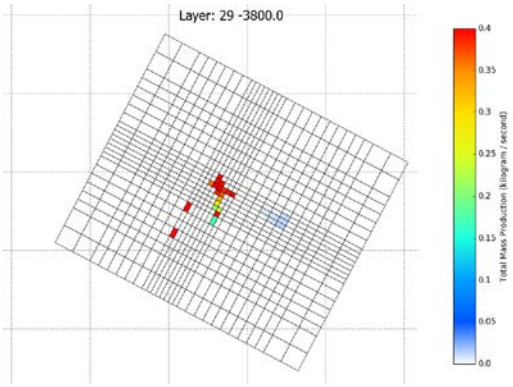

Figure 19: Post-calibration deep upflow of hot water

The temperature distribution at 1500 mbsl is shown in Figure 20. It shows that in the model the hot spot is somewhat west of that given by Ryan and Shalev (see Figure 6). This is an expected result given that the upflow under St.George's Hill is not constrained by the data.

To improve on this aspect of the model calibration would require the incorporation of the temperature model suggested by Ryan and Shalev into the suite of observations used by iTOUGH2 to calibrate the model.

Figure 21 shows the temperatures on the layer in the model just above sea level. The outflow of warm water in the west matches the location of hot water pond and hot springs north of Plymouth (see Figure 22).

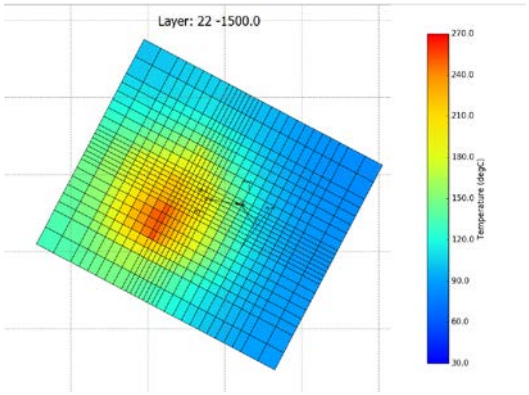

Figure 20: Temperature distribution at 1500 mbsl for calibrated model.

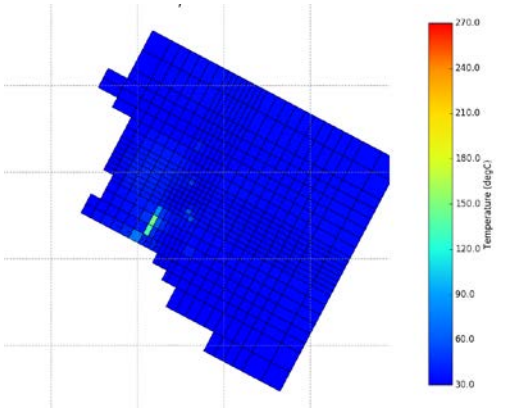

Figure 21: Temperature distribution at 25 masl for calibrated model.

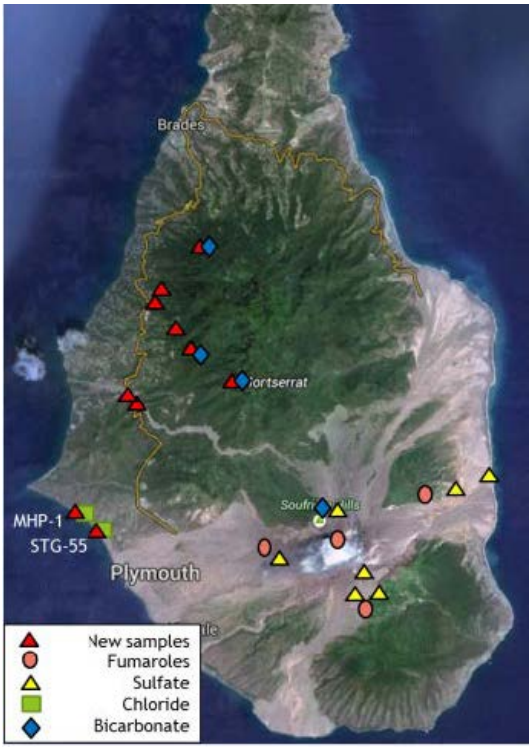

Figure 22: Geochemical Sampling Map for Montserrat (EGS, 2010).

Figure 23 shows a SW-NE slice through the model, close to wells Mon-1 and Mon2. It shows the expected upflow near the wells. Figure 24 shows an NW-SE slice through the model. In this case the upflow may be too far towards the NW and perhaps should be centred more under St. George's Hill (the highest peak on this section).

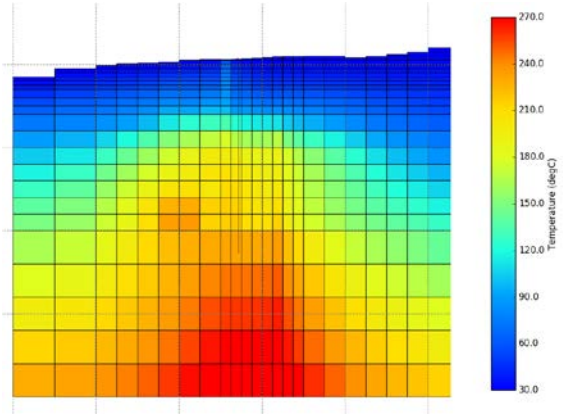

Figure 23: Temperature distribution on a SW-NE slice for the calibrated model.

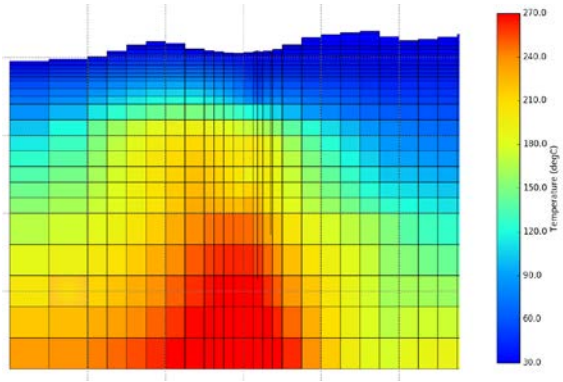

Figure 24: Temperature distribution on a NW-SE slice for the calibrated model.

5. CONCLUSION

With the aid of iTOUGH2 it was possible to calibrate a natural state model of Montserrat geothermal system to very well match the observed temperature profiles for Mon-1 and Mon-2. However the limited data do not constrain some of the permeability structure of the model very well and the hot reservoir in the computer model may be too far west. In future work we will include temperatures inferred from the seismic tomography study of Ryan and Shalev (2014) in the suite of observation data to be matched.

ACKNOWLEDGEMENTS

We would like to thank The Department for International development and the Government of Montserrat for funding aspects of this work and for allowing the use of geothermal drilling and exploration data. We would also like to acknowledge the Campus Research and Publication Fund of The University of the West Indies (CRP.3.JUN15.13) for access to funding as well.

REFERENCES

Croucher, A.E.: PyTOUGH: a Python scripting library for automating TOUGH2 simulations, *Proc. 33rd New Zealand Geothermal Workshop*, Auckland, New Zealand. (2011).

Croucher, A. E.: Recent developments in the PyTOUGH scripting library for TOUGH2 simulations. *Proc. 37th New Zealand Geothermal Workshop*. Taupo, New Zealand. (2015).

EGS Inc.: Geothermal Exploration in Montserrat, Caribbean, EGS Inc., Final Report. *Prepared for the Minister of Communications and Works, Government of Montserrat, Caribbean*, 1-11 (2010).

Finsterle, S.: *iTOUGH2 User's Guide*, Report LBNL-40040, Earth Sciences Division Lawrence Berkeley National Laboratory, University of California, Berkeley, CA 94720, USA. 137 p. (2007).

Harford, C.L., Pringle, M.S., Sparks, R.S.J. and Young, S. R.: The volcanic evolution of Montserrat using 40Ar/ 39Ar geochronology, *in* T. H. Druitt and B. P. Kokelaar, eds., The eruption of the Soufrière Hills Volcano, Montserrat, from 1995 to 1999: *Geological Society*, 21, 93-113 (2002).

Jaud, P. and Lamethe, D.: The Bouillante geothermal power-plant, Guadeloupe. *Geothermics* 14 (2), 197-205 (1985).

Rowland, J., and G. Ryan. 2014. Structural Architecture of St George's Hill & Surrounds: Implications for geothermal well siting. Auckland: Auckland Uniservices Ltd.

Ryan, G.A., Peacock, J.R., Shalev, E. and Rugis, J.: Montserrat geothermal system: a 3D conceptual model. *Geophysical Research Letters*, 40, 1-6 (2013).

Ryan, G. A. and Shalev, E.: Seismic Velocity/Temperature Correlations and a Possible New Geothermometer: Insights from Exploration of a High-Temperature Geothermal System on Montserrat, West Indies. *Energies* 7 (10), 6689-6720 (2014).

Sumantoro, Z.Z.: Reservoir modelling of the geothermal system in Montserrat. *Geothermal Project Report*, Geothermal Institute, University of Auckland (2014).

Wadge, G., Voight, B., Sparks, R.S.J., Cole, P.D., Loughlin, S.C. and Robertson, R.E.A.: Chapter 1 An overview of the eruption of Soufrière Hills Volcano, Montserrat from 2000 to 2010. *Geological Society, London, Memoirs* 39 (1), 1-40 (2014).

Wellmann, J. F., Croucher, A.E. & Regenauer-Lieb, K.: Python scripting libraries for subsurface fluid and heat flow simulations with TOUGH2 and SHEMAT, *Computers & Geosciences*, 43, 197-206 (2012).